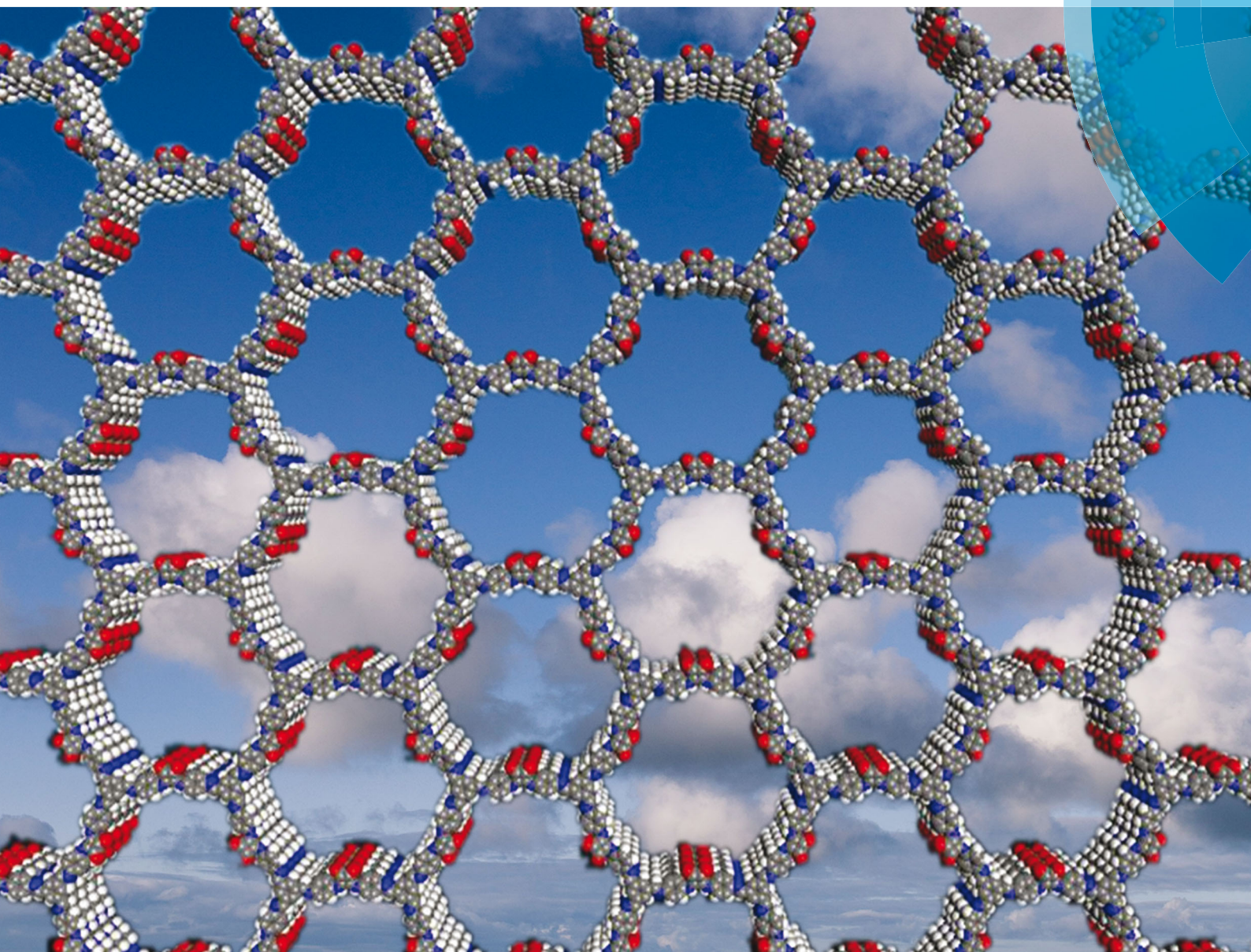


ChemComm

Chemical Communications

rsc.li/chemcomm



ISSN 1359-7345



ROYAL SOCIETY
OF CHEMISTRY

Celebrating
IYPT 2019

COMMUNICATION

Shengqian Ma, Yao Chen, Zhenjie Zhang *et al.*
Squaramide-decorated covalent organic framework
as a new platform for biomimetic hydrogen-bonding
organocatalysis

Cite this: *Chem. Commun.*, 2019, 55, 5423Received 15th February 2019,
Accepted 1st April 2019

DOI: 10.1039/c9cc01317b

rsc.li/chemcomm

Squaramide-decorated covalent organic framework as a new platform for biomimetic hydrogen-bonding organocatalysis†

Xia Li,^a Zhifang Wang,^a Jiaying Sun,^b Jia Gao,^a Yu Zhao,^a Peng Cheng,^{id} ^{ab}
Briana Aguila,^{id} ^c Shengqian Ma,^{id} ^{*c} Yao Chen^{id} ^{*b} and Zhenjie Zhang^{id} ^{*abd}

A squaramide-decorated COF was synthesized and used as a highly efficient heterogeneous catalyst for hydrogen-bonding organocatalysis as exemplified in the context of catalyzing Michael addition reactions under mild conditions. Our work lays a foundation for the development of functional COFs as a new platform for biomimetic organocatalysis.

Covalent organic frameworks (COFs) are a class of designable crystalline polymers with structural periodicity and inherent porosity that consist of cross-linked organic building blocks.¹ Benefiting from their high crystallinity,² tunable pore size³ and large surface area,⁴ COFs demonstrate diverse applications including gas storage,⁵ gas separation,⁶ catalysis,⁷ smart sensors,⁸ optoelectronics,⁹ drug delivery,¹⁰ energy storage¹¹ and so on. Recently, the exploration of COFs as heterogeneous catalysts has attracted increasing attention due to the high catalytic efficiency, excellent stability and good reusability.¹² One routine strategy to construct COF catalysts is incorporating catalytic metal particles or organic species into COFs *via* post-synthetic modifications. For example, Wang *et al.* immobilized Pd species into **COF-LZU1** to catalyze Suzuki–Miyaura Coupling reactions.¹³ Another alternate strategy is using catalytic monomers to directly prepare COFs in which the framework itself is catalytic. Yaghi and co-workers used porphyrins as monomers to prepare porphyrin COFs with high efficiency for electrocatalytic carbon dioxide reduction.¹⁴ Cui *et al.* synthesized a

series of BINOL-based COFs to catalyze asymmetric addition reactions of diethylzinc to aldehydes.¹⁵

Hydrogen-bonding organocatalysis has been developed as excellent biomimetic alternatives to Lewis acid catalysis.¹⁶ Recently, bifunctional squaramide moieties have been proven as excellent biomimetic hydrogen-bonding organocatalysts,¹⁷ ascribed to their hydrogen-bond accepting and donating functionality through their carbonyl and N–H groups, respectively.¹⁸ Structurally, squaramides are related to the arginine residue *via* their relationship to the urea and guanidinium ion.¹⁹ However, due to the strong intermolecular hydrogen-bonding interactions between carbonyl and N–H groups,²⁰ squaramide derivatives suffer from severe self-association/aggregation that seriously hinders squaramides' solubility and catalytic efficiency.²¹ To tackle this issue, one facile and effective strategy is to incorporate squaramide moieties into porous materials to form heterogeneous catalysts, which can offer many advantages such as good reusability and enhanced stability.⁷ For instance, squaramide-based carboxylic ligands have been used to construct porous metal–organic frameworks (MOFs) to serve as effective heterogeneous catalysts towards Friedel–Crafts reactions.²¹ However, to the best of our knowledge, there is no report for squaramide-based COFs up to now. Herein, we created a catalytic squaramide-linked COF with good crystallinity and high porosity. Moreover, this novel COF can catalyze Michael addition reactions with high catalytic efficiency and good reusability. This study not only enriches the library of COF materials, but also points out a new strategy to design and synthesize heterogeneous biomimetic organocatalysts.

In order to construct squaramide-linked COFs, we first designed and synthesized a new diamino monomer functionalized with a squaramide core, 3,4-bis((4 aminophenyl)amino)cyclo-but-3-ene-1,2-dione (**1**). Diffusion of CH₂Cl₂ into a DMF solution of **1** yielded yellow prism crystals of **1**. Single crystal diffraction data revealed that monomer **1** is a linear molecule, which possesses a similar shape and length as [1,1':4',1''-terphenyl]-4,4''-diamine (**3**) (Fig. S1, ESI†). The C₃-symmetric 1,3,5-triformylbenzene (**2**) was widely employed as the basic

^a College of Chemistry, Nankai University, Tianjin, 300071, China.
E-mail: zhangzhenjie@nankai.edu.cn

^b State Key Laboratory of Medicinal Chemical biology, Nankai University, Tianjin 300071, China. E-mail: chenyaoyao@nankai.edu.cn

^c Department of Chemistry, University of South Florida, 4202 E. Fowler Avenue, Tampa, Florida 33620, USA. E-mail: sqma@usf.edu

^d Key Laboratory of Advanced Energy Materials Chemistry, Ministry of Education, Nankai University, Tianjin 300071, China

† Electronic supplementary information (ESI) available: PXRD patterns, FT-IR spectra, SEM images, BET curves, catalytic details and NMR spectra. CCDC 1839497. For ESI and crystallographic data in CIF or other electronic format see DOI: 10.1039/c9cc01317b

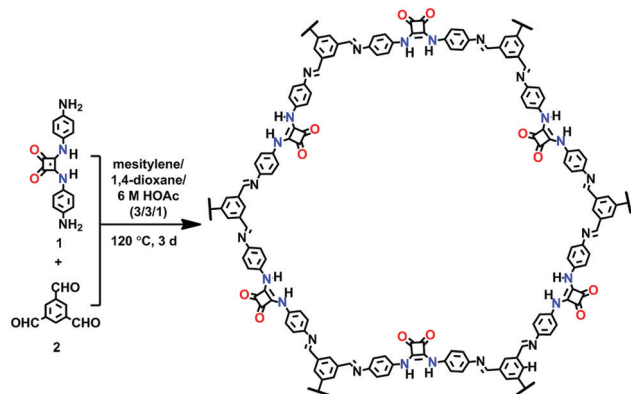


Fig. 1 Synthesis of **COF-SQ** by condensation of monomer **1** and **2**.

backbone of COFs because the rigid and triaryl benzene group is ideal for constructing COFs of large hexagonal channels (Fig. 1).¹³ For example, Lei and coworkers synthesized an imine-linked COF (**2DP**₁₊₅) of ~3.7 nm hexagonal channels *via* the condensation reaction of monomer **2** and **3**.²² Considering the similarity of **1** and **3**, we successfully prepared a squaramide-linked COF, **COF-SQ**, *via* the condensation reaction of **1** (0.15 mmol) and **2** (0.10 mmol) in a mixed solvent of mesitylene and 1,4-dioxane in the presence of 6.0 M acetic acid as catalyst within a flame-sealed glass ampule at 120 °C for 3 days. Subsequently, the as-prepared powder was collected by centrifugation or filtration and washed with THF and acetone using Soxhlet extraction for 24 h, respectively. After drying under vacuum at 120 °C, a brown-colored powder was obtained. A molecular analogue of **COF-SQ** with a squaramide core, 3,4-bis((4-(*E*)-benzylideneamino)phenyl) amino)cyclobut-3-ene-1,2-dione (**4**), was successfully synthesized and used as a model compound (Scheme S2, ESI†). The IR spectrum of **1** shows that the characteristic N–H stretching vibration at 3413 cm⁻¹ and 3286 cm⁻¹ and C=O stretching vibration of **2** at 1681 cm⁻¹ disappeared after the reaction. Meanwhile, the C=N stretching vibrations (1618 cm⁻¹) of **COF-SQ** (1622 cm⁻¹ for **4**) (Fig. S2, ESI†),²³ indicating the formation of imine bonds. The ¹³C CP-MAS NMR spectra showed the characteristic signal for the C=N and C=O groups at around 165 ppm and 181 ppm (Fig. 2), respectively. These results further confirmed the formation of imide groups in **COF-SQ**. Powder X-ray diffraction (PXRD)

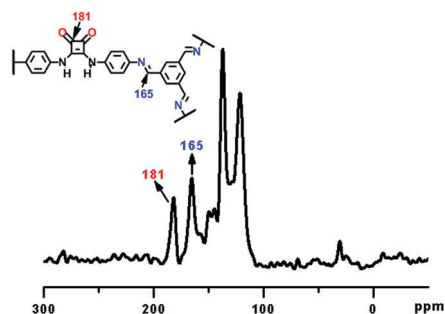


Fig. 2 ¹³C CP/MAS NMR spectra of **COF-SQ**. The assignments of ¹³C chemical shifts of **COF-SQ** were indicated in the chemical structure.

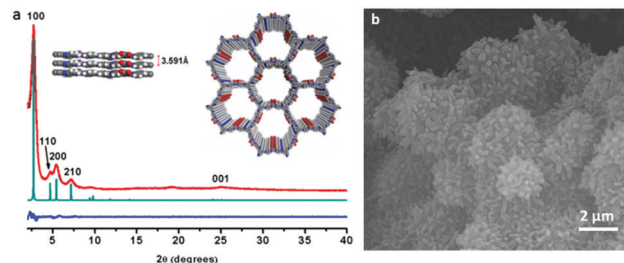


Fig. 3 PXRD patterns of the **COF-SQ** with the experimental profiles in red, Pawley-refined profiles in black, calculated profiles in green and the differences between the experimental and refined PXRD patterns in blue (Inset: views from the *b*-axis) (a). SEM image of **COF-SQ** (b).

analysis was used to determine the crystalline structure of **COF-SQ**. To resolve its crystal structure, a 3D extended sheet holding the structure as illustrated in Fig. 3a was constructed. The PXRD pattern (Fig. 3a, red) indicates that **COF-SQ** is a microcrystalline material with a long-range structure. **COF-SQ** exhibited six prominent diffraction peaks at 2.79°, 4.69°, 5.40°, 7.30° and 25.07°, corresponding to the (100), (110), (200), (210) and (001) facets, respectively. The Pawley-refined PXRD profiles matched with the experimental patterns very well (Fig. 3a and Fig. S3, ESI†). **COF-SQ** adopts the AA stacking mode of a space group of *P6* with $a = b = 37.8915 \text{ \AA}$, interlayer distance (*c*) of 3.5912 Å, $\alpha = \beta = 90^\circ$ and $\gamma = 120^\circ$ (Table S2, ESI†). Scanning electron microscopy (SEM) images of as-prepared **COF-SQ** powders showed uniformly dispersed globular particles with 140–250 nm size (Fig. 3b and Fig. S4, ESI†).

Thermal gravimetric analysis (TGA) exhibited no weight loss under N₂ atmosphere up to 380 °C (Fig. S5, ESI†). In addition, **COF-SQ** exhibited good solvent stability in common solvents, such as toluene, acetone and THF, indicated by the unchanged intensity and position of the PXRD patterns (Fig. S6, ESI†). These characteristics of **COF-SQ** are essential to heterogeneous catalysts. The porosity of **COF-SQ** was studied by measuring N₂ adsorption-desorption at 77 K on the activated samples. The adsorption curves of **COF-SQ** exhibited the classic type IV isotherm (Fig. 4), which is characteristic of mesoporous materials.²⁴ The Brunauer–Emmett–Teller (BET) and Langmuir surface area of **COF-SQ** was estimated to be 1195 m² g⁻¹ and 2014 m² g⁻¹, respectively (Fig. S7, ESI†). The nonlocal density functional theory (NLDFT) gave rise to a narrow pore size distribution with an average pore width centered at 3.6 nm, in good agreement with the related simulated value of 3.8 nm.

Traditional heterogeneous organocatalysts are mostly formed by incorporating organocatalysts into nonporous polymer supports.²⁵ However, such catalysts exhibit low activities as a result of inefficient accessibility to the catalytic sites. A promising way to circumvent this problem can turn to immobilization of the organocatalysts on porous materials including zeolites, MOFs and COFs.²⁶ The open meso-sized channels and good chemical stability of COFs would allow efficient access to the uniformly distributed organocatalyst sites and facilitate the transport of reactants and products, which may give rise to high activity in catalytic reactions.²⁷

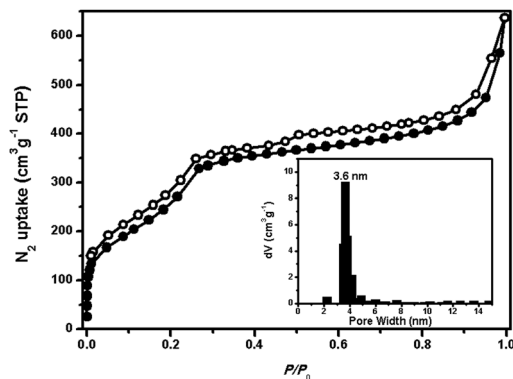


Fig. 4 Nitrogen adsorption–desorption isotherms of **COF-SQ**. (Inset) Pore size distribution of **COF-SQ**. Adsorption and desorption points are represented by filled and empty symbols, respectively.

The catalytic activity of **COF-SQ** was examined in the context of Michael addition reactions.²⁸ Michael addition reaction is one of the basic C–C bond formation reactions and provides a powerful synthetic tool for the formation of synthons of many important natural and biologically active products.²⁹ In our initial investigation, we selected β -nitrostyrene and 2,4-pentanedione as model substrates to explore the optimal reaction conditions (Table 1). Firstly, the reaction was performed using β -nitrostyrene and 2,4-pentanedione as reactants at 50 °C in toluene in the presence of 10 mol% **COF-SQ** for 24 h. The Michael addition reaction occurred and gave a yield of 95% (TON of 9.5 and TOF of 0.396 h⁻¹). To optimize the reaction conditions, we screened various solvents on this catalytic system (Fig. S8, ESI†). As summarized in Table 1, we found CH₂Cl₂ and toluene were the superior solvents in comparison with other solvents. For protic solvents such as MeOH, CH₃CN and acetone, a

Table 1 Optimization of reaction conditions for the Michael addition reaction between β -nitrostyrene and 2,4-pentanedione^a

Entry	Catalyst	Temp (°C)	Time (h)	Solvent	Yield ^b (%)
1	COF-SQ	50	24	Toluene	95
2	COF-SQ	50	24	THF	70
3	COF-SQ	50	24	Acetone	40
4	COF-SQ	50	24	CH ₂ Cl ₂	99
5	COF-SQ	50	24	CHCl ₃	76
6	COF-SQ	50	24	DMSO	88
7	COF-SQ	50	24	MeOH	33
8	COF-SQ	50	24	CH ₃ CN	79
9	COF-SQ	r.t.	24	Toluene	75
10	COF-SQ	60	24	Toluene	98
11	COF-SQ^c	50	24	Toluene	64
12	Monomer 1	50	24	Toluene	35
13	Monomer 2	50	24	Toluene	Trace
14	Model compound 4	50	24	Toluene	63
15	2DP₁₊₅	50	24	Toluene	Trace

^a Reaction condition: **1a** (0.10 mmol), **2a** (0.15 mmol), **COF-SQ** (10 mol%) in 1.0 mL solvent. ^b Determined by ¹H NMR spectroscopy of the crude mixture. ^c **COF-SQ** (5 mol%).

strong hydrogen-bonding effect may exist between the catalytic sites and protic solvent which can influence the catalytic effect.¹⁸ However, for aprotic solvents, such as CH₂Cl₂ and toluene, they won't interact with the catalytic sites of **COF-SQ**, which thus exhibited high catalytic activity. In addition, we also studied the influence of temperature to the catalytic activity of **COF-SQ**. We found the lower temperature (e.g. room temperature) gave a lower yield of 75%, while the higher temperature (60 °C) provided a similar yield (98%) as 50 °C (95%). Moreover, we explored the substrate scope of Michael addition reaction with various nucleophile and electrophile substrates as listed in Table 2. We examined the possibility to use various 1,3-dicarbonyl compounds as nucleophiles (Table 2, entries 1–4) which all formed the conjugate addition products with 98–71% yields. In addition, decent yields (92–63%) were observed for a broad range of aryl, halogenated aryl and alkyl substituted β -nitroolefins (Table 2, entries 5–8). It was found that substrate bearing electron-donating groups (Table 2, entry 5) possessed higher yields than electron-withdrawing groups on the aryl ring (Table 2, entries 6–8).¹⁶

In order to study if the catalytic activity is originated from the squaramide or other sites, monomer **1**, **2** and model compound **4**, along with **2DP₁₊₅**, which possesses a similar structure as **COF-SQ** but without squaramide moiety, were chosen as controls.³⁰ As expected, no catalytic activity was observed for **2** and **2DP₁₊₅** due to the lack of catalytic sites (Table 1, entries 12–15 and Fig. S9, ESI†).²² It is noteworthy that squaramide monomer **1** and model compound **4** possessed much lower activity than **COF-SQ**. These results indicate that the high porosity of **COF-SQ** and uniformly distributed catalytic sites may contribute to the high activity of **COF-SQ**. To further explore the advantage of heterogeneous catalyst, we tested the reusability of **COF-SQ** and found it could be easily recovered by centrifugation and reused for at least 4 times without significant loss of catalytic activity (Fig. S10, ESI†). The PXRD patterns (Fig. S11, ESI†) of the recycled **COF-SQ** revealed that its crystallinity was retained.³¹ A hot filtration test was further performed

Table 2 Michael addition reaction of various nucleophiles and electrophiles^a

Entry	R	R ¹ , R ²	Yield ^b (%)
1	(1a)H	(2a)H, H	95
2	(1a)H	(2b)H, OCH ₂ CH ₃	98
3	(1a)H	(2c)H, OCH ₃	98
4	(1a)H	(2d)CH ₃ , OCH ₃	71
5	(1b)CH ₃	(2a)H, H	92
6	(1c)OCH ₃	(2a)H, H	74
7	(1d)Cl ^c	(2a)H, H	63
8	(1e)Br	(2a)H, H	73

^a Reactions were performed with the electrophile (0.10 mmol) and the nucleophile (0.15 mmol) in the presence of catalyst (10 mol%) in toluene (1.0 mL) at 50 °C for 24 h. ^b Isolated yield determined by ¹H NMR spectroscopy of the crude mixture. ^c (*E*)-1-Chloro-3-(2-nitrovinyl)benzene.

to study the heterogeneous catalyst nature for **COF-SQ** (Fig. S12, ESI†). We found the catalysis reaction was stopped once **COF-SQ** catalyst was removed from the reaction mixture by hot filtration, suggesting **COF-SQ** indeed catalyzed the reaction. These results verified the heterogeneous nature of **COF-SQ** as a catalyst.²¹

In summary, we developed a straightforward strategy for the construction of catalytic squaramide-linked COFs (**COF-SQ**) via direct employment of catalytic squaramide building blocks. **COF-SQ** exhibited high crystallinity, permanent porosity and good thermal/solvent stability. Moreover, **COF-SQ** demonstrated good catalytic performance and good recyclability compared to the homogeneous counterparts in Michael addition reaction. Our discovery paves a new way for the construction of squaramide-based heterogeneous catalysts and broadens the highly-valued applications of functional COFs. Further investigations regarding the design and synthesis of new catalytic COFs toward high value-added reactions are ongoing in our lab.

The authors acknowledge the financial support from the National Natural Science Foundation of China (21601093).

Conflicts of interest

There are no conflicts to declare.

Notes and references

- (a) N. Huang, P. Wang and D. Jiang, *Nat. Rev. Mater.*, 2016, **1**, 16068; (b) C. S. Diercks and O. M. Yaghi, *Science*, 2017, **355**, 923; (c) Y. Jin, Y. Hu and W. Zhang, *Nat. Rev. Chem.*, 2017, **1**, 0056.
- (a) D. Beaudoin, T. Maris and J. D. Wuest, *Nat. Chem.*, 2013, **5**, 830–834; (b) G. Lin, H. Ding, D. Yuan, B. Wang and C. Wang, *J. Am. Chem. Soc.*, 2016, **138**, 3302–3305; (c) X. Han, J. Huang, C. Yuan, Y. Liu and Y. Cui, *J. Am. Chem. Soc.*, 2018, **140**, 892–895.
- (a) S. Das, P. Heasman, T. Ben and S. Qiu, *Chem. Rev.*, 2017, **117**, 1515–1563; (b) S. Karak, S. Kumar, P. Pachfule and R. Banerjee, *J. Am. Chem. Soc.*, 2018, **140**, 5138–5145.
- (a) Q. Fang, Z. Zhuang, S. Gu, R. B. Kaspar, J. Zheng, J. Wang, S. Qiu and Y. Yan, *Nat. Commun.*, 2014, **5**, 4503; (b) R. P. Bisbey and W. R. Dichtel, *ACS Cent. Sci.*, 2017, **3**, 533–543; (c) Y. Yang, X. Zou, P. Cui, Y. Zhou, S. Zhao, L. Wang, Y. Yuan and G. Zhu, *ACS Appl. Mater. Interfaces*, 2017, **9**, 30958–30963.
- Y. Zeng, R. Zou and Y. Zhao, *Adv. Mater.*, 2016, **28**, 2855–2873.
- (a) N. Huang, L. Zhai, H. Xu and D. Jiang, *J. Am. Chem. Soc.*, 2017, **139**, 2428–2434; (b) K. Dey, M. Pal, K. C. Rout, H. S. Kunjattu, A. Das, R. Mukherjee, U. K. Kharul and R. Banerjee, *J. Am. Chem. Soc.*, 2017, **139**, 13083–13091.
- (a) H. Xu, J. Gao and D. Jiang, *Nat. Chem.*, 2015, **7**, 905–912; (b) Q. Sun, B. Aguila, J. A. Perman, N. Nguyen and S. Ma, *J. Am. Chem. Soc.*, 2016, **138**, 15790–15796; (c) S. Lu, Y. Hu, S. Wan, R. McCaffrey, Y. Jin, H. Gu and W. Zhang, *J. Am. Chem. Soc.*, 2017, **139**, 17082–17088; (d) Q. Sun, C. W. Fu, B. Aguila, J. Perman, S. Wang, H. Y. Huang, F. S. Xiao and S. Ma, *J. Am. Chem. Soc.*, 2018, **140**, 984–992.
- (a) N. Huang, X. Ding, J. Kim, H. Ihee and D. Jiang, *Angew. Chem., Int. Ed.*, 2015, **127**, 8828–8831; (b) Q. Sun, B. Aguila, L. D. Earl, C. W. Abney, L. Wojtas, P. K. Thallapally and S. Ma, *Adv. Mater.*, 2018, 1705479.
- (a) M. Calik, F. Auras, L. M. Salonen, K. Bader, I. Grill, M. Handloser, D. D. Medina, M. Dogru, F. Lobermann, D. Trauner, A. Hartschuh and T. Bein, *J. Am. Chem. Soc.*, 2014, **136**, 17802–17807; (b) P. F. Wei, M. Z. Qi, Z. P. Wang, S. Y. Ding, W. Yu, Q. Liu, L. K. Wang, H. Z. Wang, W. K. An and W. Wang, *J. Am. Chem. Soc.*, 2018, **140**, 4623–4631; (c) B. Nath, W. H. Li, J. H. Huang, G. E. Wang, Z. H. Fu, M. S. Yao and G. Xu, *CrystEngComm*, 2016, **18**, 4259–4263.
- (a) Q. Fang, J. Wang, S. Gu, R. B. Kaspar, Z. Zhuang, J. Zheng, H. Guo, S. Qiu and Y. Yan, *J. Am. Chem. Soc.*, 2015, **137**, 8352–8355; (b) S. Mitra, H. S. Sasmal, T. Kundu, S. Kandambeth, I. Kavya, D. Diaz and R. Banerjee, *J. Am. Chem. Soc.*, 2017, **139**, 4513–4520.
- (a) C. R. DeBlase, K. E. Silberstein, T. T. Truong, H. D. Abruna and W. R. Dichtel, *J. Am. Chem. Soc.*, 2013, **135**, 16821–16824; (b) S. Wang, Q. Wang, P. Shao, Y. Han, X. Gao, L. Ma, S. Yuan, X. Ma, J. Zhou, X. Feng and B. Wang, *J. Am. Chem. Soc.*, 2017, **139**, 4258–4261.
- E. L. Spitzer and W. R. Dichtel, *Nat. Chem.*, 2010, **2**, 672–677.
- (a) S. Y. Ding, J. Gao, Q. Wang, Y. Zhang, W. G. Song, C. Y. Su and W. Wang, *J. Am. Chem. Soc.*, 2011, **133**, 19816–19822; (b) J. L. Segura, M. J. Mancheno and F. Zamora, *Chem. Soc. Rev.*, 2016, **45**, 5635–5671.
- C. S. Diercks, S. Lin, N. Kornienko, E. A. Kapustin, E. M. Nichols, C. Zhu, Y. Zhao, C. J. Chang and O. M. Yaghi, *J. Am. Chem. Soc.*, 2018, **140**, 1116–1122.
- X. Wang, X. Han, J. Zhang, X. Wu, Y. Liu and Y. Cui, *J. Am. Chem. Soc.*, 2016, **138**, 12332–12335.
- (a) J. P. Malerich, K. Hagihara and V. H. Rawal, *J. Am. Chem. Soc.*, 2008, **130**, 14416–14417; (b) J. V. Alegre-Requena, E. Marqués-López, R. P. Herrera and D. D. Díaz, *CrystEngComm*, 2016, **18**, 3985–3995.
- (a) R. I. Storer, C. Aciro and L. H. Jones, *Chem. Soc. Rev.*, 2011, **40**, 2329–2346; (b) R. S. Tikhvatshin, A. S. Kucherenko, Y. V. Nelyubina and S. G. Zlotin, *ACS Catal.*, 2017, **7**, 2981–2989.
- S. M. Cohen, Z. Zhang and J. A. Boissonnault, *Inorg. Chem.*, 2016, **55**, 7281–7290.
- F. Olmo, C. Rotger, I. Ramírez-Macías, L. Martínez, C. Marín, L. Carreras, K. Urbanová, M. Vega, G. Chaves-Lemauro, A. Sampedro, M. J. Rosales, M. Sánchez-Moreno and A. Costa, *J. Med. Chem.*, 2014, **57**, 987–999.
- G. Kardos and T. Soós, *Eur. J. Org. Chem.*, 2013, 4490–4494.
- X. Zhang, Z. Zhang, J. Boissonnault and S. M. Cohen, *Chem. Commun.*, 2016, **52**, 8585–8588.
- Y. Yu, J. Lin, Y. Wang, Q. Zeng and S. Lei, *Chem. Commun.*, 2016, **52**, 6609–6612.
- D. N. Bunck and W. R. Dichtel, *J. Am. Chem. Soc.*, 2013, **135**, 14952–14955.
- J. Zhang, X. Han, X. Wu, Y. Liu and Y. Cui, *J. Am. Chem. Soc.*, 2017, **139**, 8277–8285.
- (a) E. A. Hall, L. R. Redfern, M. H. Wang and K. A. Scheidt, *ACS Catal.*, 2016, **6**, 3248–3252; (b) Q. Fang, S. Gu, J. Zheng, Z. Zhuang, S. Qiu and Y. Yan, *Angew. Chem., Int. Ed.*, 2014, **53**, 2878–2882; (c) K. Titov, D. B. Eremin, A. S. Kashin, R. Boada, B. E. Souza, C. S. Kelley, M. D. Frogley, G. Cinque, D. Gianolio, G. Cibin, S. Rudić, V. P. Ananikov and J. C. Tan, *ACS Sustainable Chem. Eng.*, 2019, **7**, 5875–5885; (d) C. A. Wang, Z. K. Zhang, T. Yue, Y. L. Sun, L. Wang, W. D. Wang, Y. Zhang, C. Liu and W. Wang, *Chem. – Eur. J.*, 2012, **18**, 6718–6723.
- (a) H. S. Xu, S. Y. Ding, W. K. An, H. Wu and W. Wang, *J. Am. Chem. Soc.*, 2016, **138**, 11489–11492; (b) H. Xu, X. Chen, J. Gao, J. Lin, M. Addicoat, S. Irlé and D. Jiang, *Chem. Commun.*, 2014, **50**, 1292–1294; (c) J. Zhang, X. Han, X. Wu, Y. Liu and Y. Cui, *J. Am. Chem. Soc.*, 2017, **139**, 8277–8285.
- U. Díaz and A. Corma, *Coord. Chem. Rev.*, 2016, **311**, 85–124.
- W. Yang and D. M. Du, *Org. Lett.*, 2010, **12**, 5450–5453.
- H. Y. Bae, S. Some, J. S. Oh, Y. S. Lee and C. E. Song, *Chem. Commun.*, 2011, **47**, 9621–9623.
- (a) Y. Liu, C. S. Diercks, Y. Ma, H. Lyu, C. Zhu, S. A. Alshimiri, S. Alshihri and O. M. Yaghi, *J. Am. Chem. Soc.*, 2019, **141**, 677–683; (b) A. Dirksen, T. M. Hackeng and P. E. Dawson, *Angew. Chem., Int. Ed.*, 2006, **45**, 7581–7584.
- S. Y. Ding and W. Wang, *Chem. Soc. Rev.*, 2013, **42**, 548–568.